Effects of Site-Specific Acetylation on ω-Conotoxin GVIA Binding and Function

Richard A. Lampe,*,‡ Mathew M. S. Lo,‡ Richard A. Keith,‡ Michael B. Horn,‡ Michael W. McLane,‡ Joseph L. Herman,§ and Russell C. Spreen§

Departments of CNS Pharmacology and Structural Chemistry, ICI Pharmaceuticals Group, A Business Unit of ZENZCA Inc., Wilmington, Delaware 19897

Received September 29, 1992; Revised Manuscript Received January 22, 1993

ABSTRACT: Chemical modification of ω-conotoxin GVIA (ω-CgTX GVIA) was performed using nonsaturating concentrations of acetic anhydride to generate seven distinct derivatives. Following separation of these peptides using reverse-phase HPLC (RP-HPLC), their individual molecular weights were determined using fast bombardment mass spectrometry (FAB-MS). Three peptides contained a single acetylated amino group, three possessed two acetylated amino groups, and the last contained three acetylations. For each peptide, the specific site of acetylation was confirmed using a scheme of tryptic digestion, under nonreducing conditions, followed by RP-HPLC and FAB-MS. Biological profiles for each peptide were obtained by analyzing their capacity to displace native ^{125}I-ω-CgTx GVIA binding to rat hippocampal membranes and to block K^+-stimulated $^{45}Ca^{2+}$ influx into chick brain synaptosomes. The data indicate that successive additions of acetyl moieties to ω-CgTx GVIA lead to a loss of both binding affinity and Ca^{2+} influx inhibitory potency. Within the monoacetylated series, acetylation of the amino terminal of Cys-1, as compared to the ε-amino group of either Lys-2 or Lys-24, leads to the greatest shift in potency. In summary, these results indicate that basic (i.e., primary amino) groups, which are brought into close proximity as a result of disulfide bridging, are important in the functional blockade of neuronal Ca^{2+} channels by ω-CgTx GVIA.

Venom from the fish-hunting cone snail species *Conus geographus* contains a family of highly homologous, basic peptides known as ω-conotoxins (ω-CgTx)[1] that block voltage-dependent Ca^{2+} channels (VDCC) (Olivera et al., 1984, 1990; Cruz et al., 1988). ω-Conotoxin GVIA (ω-CgTx GVIA), the best characterized member of this family, is a 27 amino acid (aa) peptide containing hydroxylated prolines, an amidated carboxy terminus, and 3 intramolecular disulfide bonds with the following linkage: 1–16, 8–19, and 15–26 (Olivera et al., 1984; Nishiuchi et al., 1986). Initial functional studies indicated that ω-CgTx GVIA is a potent, irreversible blocker of a subclass of VDCC as defined by its species- and tissue-dependent blockade (Cruz & Olivera, 1986; Reynolds et al., 1986; Cruz et al., 1987; McCleskey et al., 1987; Kasai et al., 1987; Suszkiw et al., 1987). Specifically, ω-CgTx GVIA selectively interacts with neuronal versus nonneuronal VDCC and preferentially blocks the influx of Ca^{2+} into avian, amphibian, and fish nerve terminals versus mammalian nerve terminals [for a review, see Cruz et al. (1988)]. Within mammalian tissues, both peripheral and central nerve terminals contain ω-CgTx GVIA-sensitive sites as demonstrated by the potent blockade of norepinephrine release from rat sympathetic neurons (Hirning et al., 1988) and from rat brain slices (Dooley et al., 1987; Keith et al., 1989). Similarly, whole cell Ca^{2+} measurements indicate that ω-CgTx GVIA blocks VDCC associated with central as well as peripheral cell bodies although larger effects are observed peripherally. Evidence of further selectivity has been obtained from studies demonstrating that ω-CgTx GVIA specifically blocks N-type Ca^{2+} current without obvious effects on T-, L-, or P-type currents (Plummer et al., 1989; Aosaki & Kasai, 1989; Mintz et al., 1992). Binding studies performed with forskolin-differentiated NG108-15 neuroblastoma cells indicate that ω-CgTx GVIA binds to two sites with differential affinity (Werth et al., 1991). Furthermore, differentiated PC12 cells contain a residual N-type Ca^{2+} current following irreversible inhibition by ω-CgTx GVIA which is reversibly inhibited by the toxin (Plummer et al., 1989).

In conjunction with studies designed to better characterize the pharmacological specificity of ω-CgTx GVIA, attempts have been made to either identify or design smaller molecules that mimic the function of this peptide. Due to the three intramolecular disulfide bridges, the secondary structure of ω-CgTx GVIA is highly constrained. Three-dimensional molecular models of this constrained structure have been developed by us to determine the exact position of specific amino acid residues. In an attempt to extract information from these models, structure–activity profiles have to be generated following manipulations to the ω-CgTx GVIA structure. This study presents data documenting the structural and biological effects observed following brief exposure of ω-CgTx GVIA to nonsaturating quantities of acetic anhydride. It was hoped that under these conditions acetylation of the three primary amino moieties associated with Lys-2, Lys-24, and N-terminal Cys would be obtained. These primary amino moieties were felt to be important to the function of ω-CgTx GVIA because of two observations. First, ω-CgTx GVIA and other ω-CgTx are basic peptides. Second, we have observed that aminoglycoside antibiotics (i.e., neomycin, gentamycin, and kanamycin) and polyamines (i.e., spermine and spermidine) are capable of interacting with the ω-CgTx GVIA binding site and blocking the function of VDCC (Keith et al., 1990, 1992; Pullan et al., 1990). Similarly, neomycin has been shown to inhibit the specific binding of ^{125}I-ω-CgTx GVIA (Knaus et al., 1987; Wagner et al., 1988; Stumpo et al., 1991).

‡ Department of CNS Pharmacology.
§ Department of Structural Chemistry.

[1] Abbreviations: ω-CgTx GVIA, ω-conotoxin GVIA; FAB-MS, fast atom bombardment mass spectrometry; RP-HPLC, reverse-phase high-performance liquid chromatography; VDCC, voltage-dependent Ca^{2+} channels; TFA, trifluoroacetic acid; Tris, tris(hydroxymethyl)aminomethane; HEPES, *N*-(2-hydroxyethyl)piperazine-*N*′-2-ethanesulfonic acid; BSA, bovine serum albumin; KRB, Krebs–Ringer buffer; SAR, structure–activity relationship; Ac, acetylation.

0006-2960/93/0432-3255$04.00/0

EXPERIMENTAL PROCEDURES

Materials. ω-CgTx GVIA was purchased from Penisula Labs, Inc., Belmont, CA. Sequencing-grade trypsin was obtained from Boehringer Mannheim, Inc., Indianapolis, IN. ^{125}I-ω-CgTx GVIA and $^{45}Ca^{2+}$ were purchased from NEN/DuPont, Inc., Boston, MA. All other chemicals used were either HPLC or reagent grade.

Reverse-Phase HPLC (RP-HPLC). Reverse-phase HPLC (RP-HPLC) was performed using a Zorbax Rx-C8 analytical (15 cm × 4.6 mm) column purchased from Rockland Technologies, Inc., West Chester, PA. All separations were done using a 1 mL/min flow rate of the following mobile phase: buffer A, 0.1% TFA/H_2O; buffer B, 0.1% TFA/CH_3-CN. Detection of eluting peptides was monitored via UV spectroscopy at 215 nm. Concentrations of individual derivatives were deduced by calculating peak areas of the 215-nm signal and then normalizing these values against the signal obtained for a known concentration of native ω-CgTx GVIA. A complete UV spectrum was obtained for several derivatives to ascertain whether the 274-nm (λ_{max} Tyr) signal was in accordance with that obtained at 215 nm.

Acetylation. Acetic anhydride, diluted in methanol, was added directly to lyophilized ω-CgTx GVIA at a 1:1 molar ratio, allowed to react for 60 s prior to addition of 0.33 volume of H_2O, and then dried to completeness. Following resuspension in 0.1% TFA/H_2O, the acetylated sample was applied to the C8 RP-HPLC column (H_2O/CH_3CN gradient; 90:10–70:30 over 20 min with a 2.5-min delay). Individual peaks were collected, vacuum-dried, and then submitted for FAB-MS analysis to determine the incorporation of acetyl moieties. Stoichiometric adjustment of the acetic anhydride:ω-CgTx GVIA molar ratio to 1.5:1 was performed in certain cases to increase the yields of the di- and triacetylated derivatives.

Tryptic Digestion of Acetylated Derivatives. Proteolysis was performed by dissolving 50 μg of substrate into 100 μL of 100 mM Tris/20 mM $CaCl_2$ buffer (pH 7.8) that contained trypsin at a 50:1 molar ratio of substrate to enzyme. Incubations were carried out at 37 °C for 16 h. For each digestion, the major tryptic fragment was collected following RP-HPLC (H_2O/CH_3CN; 100:0–60:40 over 40 min with a 2.5-min delay), vacuum-dried, and then resuspended in 10 μL of 0.1% TFA/H_2O for MS analysis.

Fast Atom Bombardment Mass Spectrometry. Mass spectral analysis was performed on a VG 70-VSE magnetic sector mass spectrometer at 1000 resolution. Ions were produced by fast atom bombardment using 8-kV xenon atoms. The distribution of positive ions sputtered from a sample/matrix-coated stainless-steel surface was measured. The matrix consisted of 3:1 dithiothreitol/dithioerythritol (magic bullet).

^{125}I-ω-CgTx GVIA Binding Assay. ^{125}I-ω-CgTx GVIA binding to fresh crude hippocampal synaptic membranes (10 μg of protein per assay) was performed as previously described by Stumpo et al. (1991) and modified from Abe et al. (1986). Individual test compounds (i.e., acetylated ω-CgTx GVIA derivatives) were preincubated with the hippocampal membrane tissue in 5 mM HEPES/Tris buffer, pH 7.4, for 30 min prior to the addition of 20 pM ^{125}I-ω-CgTx GVIA. Following incubation for 30 min at 24 °C, the reaction mixture was filtered through glass fiber filters using a Skatron cell harvester. Filters were rinsed twice with 5 mM HEPES (pH 7.4), 150 mM NaCl, and 0.2% BSA buffer. Nonspecific binding was defined as that remaining in the presence of 100 nM ω-CgTx GVIA.

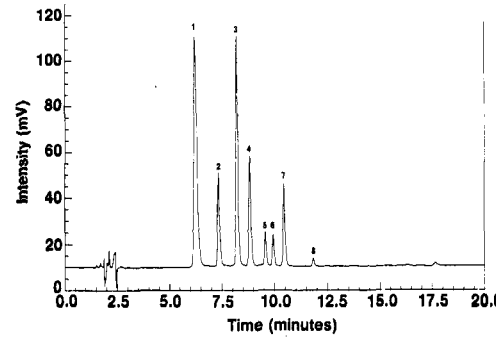

FIGURE 1: Reverse-phase HPLC chromatogram of acetylated ω-CgTx GVIA. The acetylation reaction was conducted using a 1:1 molar ratio of acetic anhydride to ω-CgTx GVIA. Separation was performed as described in the text with detection at 215 nm (0.2 absorbance unit = 1 V).

K^+-Stimulated $^{45}Ca^{2+}$ Influx into Chick Synaptosomes (P2 Pellets). Synaptosomes (P2 pellets) were prepared from whole chick brain as basically described by Reynolds et al. (1986) for rat brain tissue. Briefly, tissue was homogenized in 9 volumes of 0.32 M sucrose using a loose-fitting motor-driven Teflon–glass homogenizer. The supernatant from a 1000*g* spin (10 min) was diluted 1:1 with a Krebs–Ringer buffer (KRB) containing choline chloride substituted for NaCl (composition in millimolar:choline chloride, 140; KCl, 5; $MgCl_2$, 1.3; glucose, 10; Na-HEPES, 10; pH 7.45; aerated with O_2 for 60 min) prior to centrifugation at 10000*g* for 15 min. Resuspension of the pellet was done in 3 mL of KRB/g wet weight of tissue with gentle (5 strokes) homogenization. Synaptosomes (50 μL/tube) were kept on ice for 30 min during which time the ω-CgTx GVIA derivatives were preequilibrated with the tissue. $^{45}Ca^{2+}$ influx was initiated by the addition of 450 μL of either low (5 mM) or high (50 mM; isoosmotic substitution with choline chloride) K^+-containing KRB spiked with approximately 2 μCi/mL $^{45}Ca^{2+}$/1 mM $CaCl_2$. Rapid quenching of the influx, following a 1-s incubation period, was accomplished by adding 3 mL of KRB that contained 10 mM NaEGTA isoosmotically substituted for choline chloride. Samples were immediately filtered through Whatman GF/C glass fiber filters using a Hoefer FH225V filtration instrument. Filters were washed with 3 × 4 mL of wash KRB (composition in millimolar:choline chloride, 139; KCl, 5; $MgCl_2$, 1.3; $LaCl_3$, 2; glucose, 10; Na-HEPES, 10; pH 7.45) and dried at 24 °C for 16 h, and the retained radioactivity was determined by liquid scintillation spectroscopy. Net voltage-dependent $^{45}Ca^{2+}$ uptake was determined as the difference between uptake in the high-K^+ and low-K^+ KRB buffers.

RESULTS

Derivatization of ω-CgTx GVIA, using nonsaturating concentrations of acetic anhydride, generated eight distinct RP-HPLC peaks (Figure 1). The average molecular weight of the $(M + H)^+$ ion for each of the HPLC peaks is shown in Figure 2. Peak 1 contained residual, unreacted (i.e., native) ω-CgTx GVIA at m/z = 3038.1. Peaks 2–4 are shifted 42 Da higher to m/z = 3080.0, 3080.2, and 3080.3, respectively, which corresponds to a single acetylation. An additional mass shift of 42 Da (m/z = 3122.4, 3122.3, and 3122.3) was observed for peaks 5–7, indicating the presence of the diacetylated species. Peak 8, at m/z = 3164.4, contained the triacetylated derivative.

Positional assignment of the site of acetylation(s) for each modified species was accomplished using tryptic digestion, without prior disulfide reduction, followed by FAB-MS

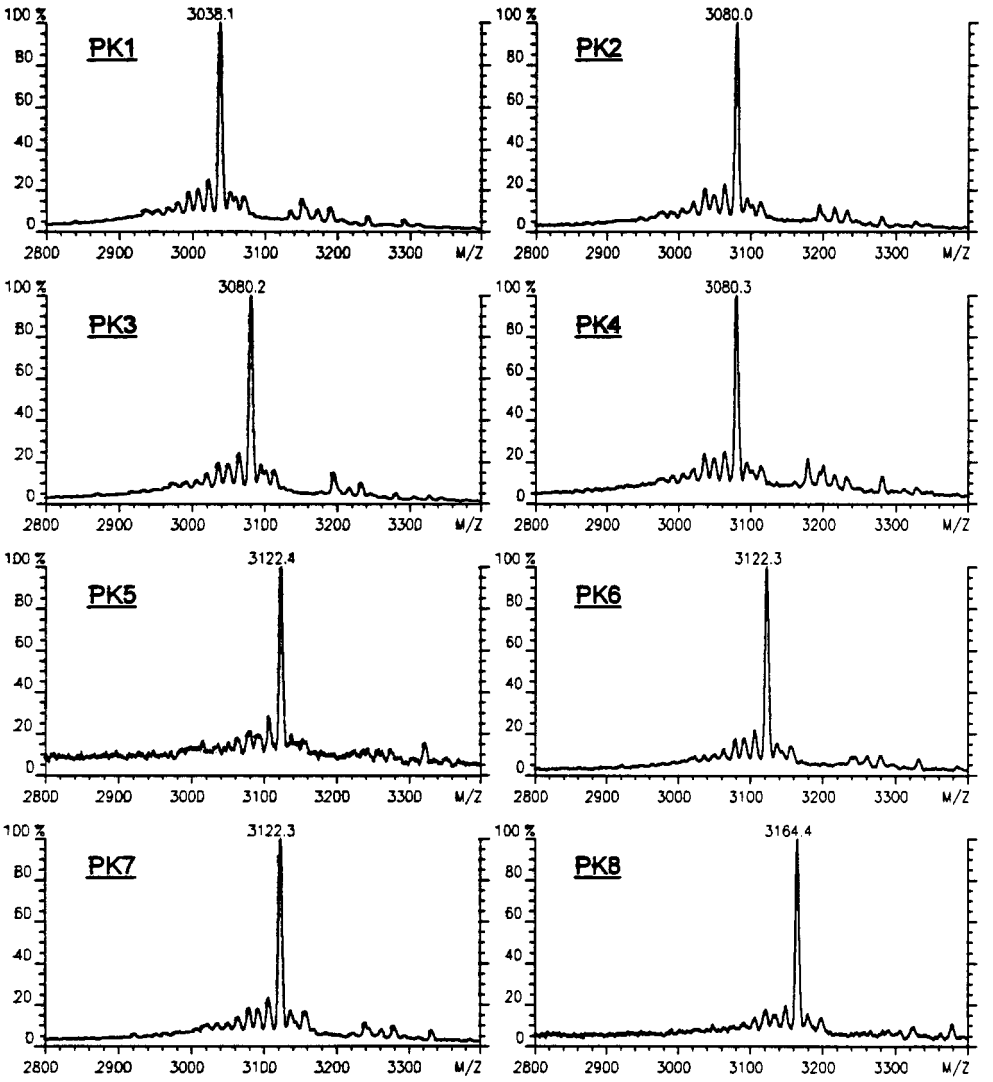

FIGURE 2: Positive ion FAB mass spectra of RP-HPLC peaks 1–8 from Figure 1. The mass signal is expressed as the relative intensity along the y axis.

analysis of the major tryptic fragment. The rationale for assignments is schematically presented in Figure 3 and is based upon the potential acetylation of the three primary amines located at the N-terminus, Lys-2 and Lys-24, the Lys-Arg sequence at positions 24–25, and the blockage of tryptic reactivity following acetylation of the Lys residues. Specifically, acetylation of the N-terminus does not interfere with cleavage of any peptide bonds and the concomitant addition of H_2O at these sites, whereas acetylation of the ϵ-NH_2 of a Lys residue will selectively prevent tryptic hydrolysis at this location. Furthermore, lack of acetylation at Lys-24 will lead to a mass decrease due to the loss of Arg-25 from the molecule. Therefore, each of the possible acetylated ω-CgTx GVIA derivatives will possess a unique molecular weight after tryptic digestion as discussed below. When the α-NH_2 of Cys-1 is acetylated, a mass of 2978.2 daltons will be observed for the $(M+H)^+$ ion which corresponds to a 42-dalton mass increase vs native, digested ω-CgTx GVIA (i.e., the same mass shift as for nondigested entities). Acetylation of the ϵ-NH_2 of Lys-2 will block tryptic cleavage at this position, and the observed mass of 2960.2 daltons will be 18 daltons lower than that determined for the NH_2-terminal acetylated species. Modification of the ϵ-NH_2 of Lys-24 will block tryptic cleavage at this position, allowing for the Arg residue at position 25 to be retained and an increase of 156 daltons (m/z = 3134.4) to be observed vs the NH_2-terminal derivative. Similarly, the diacetylated derivatives will reflect the three potential permutations available with a resultant observed mass of either 3002.2 (acetylation of the N-terminus and Lys-2), 3158.5 (acetylation of Lys-2 and Lys-24), or 3176.5 daltons (acetylation of the N-terminus and Lys-24) for the $(M+H)^+$ ion. It is essential to remember that although the ω-CgTx GVIA (i.e., each ω-CgTx GVIA derivative) molecule has undergone proteolytic cleavage, it is still a single chemically bonded entity (±Arg-25) under nonreducing conditions on the basis of the disulfide bridging.

As shown in Figure 4, the anticipated mass spectral values were obtained for the mono- and diacetylated derivatives and the definitive assignments made as follows: peak 2, acetylation of Lys-2; peak 3, acetylation of the N-terminus; peak 4, acetylation of Lys-24; peak 5, acetylation of the N-terminus and Lys-2; peak 6, acetylation of Lys-2 and Lys-24; peak 7, acetylation of the N-terminus and Lys-24. Analysis of the HPLC profile (Figure 1), in conjunction with the specific assignments, confirms that the N-terminus is acetylated to a greater extent than the ϵ-NH_2 group of either Lys residue under these reaction conditions. Consequently, the yield of peak 3 versus either peak 2 or peak 4 was consistently higher within the monoacetylated series. Within the diacetylated series, higher yields of peak 7 were obtained, and in most cases, it was very difficult to isolate the diacetylated derivative peak 6 in large quantities due to its presumed propensity to

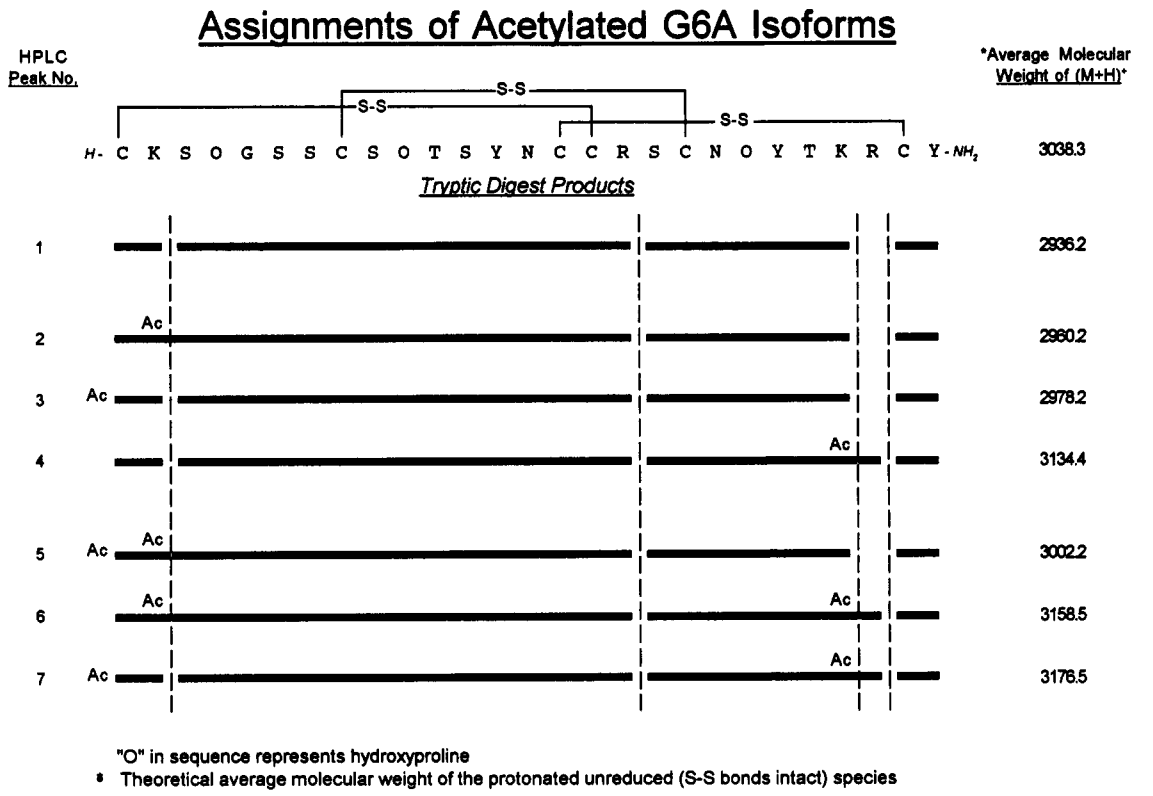

FIGURE 3: Schematic representation of the potential tryptic cleavage sites (vertical dashed lines) and the potential sites of acetylation (Ac) within ω-CgTx GVIA. At the top, the linear sequence of native, oxidized ω-CgTx GVIA is given. Mass values presented in the right-hand column are for the protonated molecular ion following tryptic digestion. The blank space between the two vertical dashed lines refers to the elimination of Arg from the molecule.

be further derivatized to the triacetylated species. Additionally, it was observed that peaks 2 and 5 were relatively more difficult to isolate vs peaks 4 and 7, indicating the ϵ-NH_2 of Lys-2 was less reactive than that of Lys-24.

To evaluate the biological significance of these modifications, each acetylated derivative was tested for its ability to inhibit the binding of ^{125}I ω-CgTx GVIA to hippocampal membranes (Figure 5). As mentioned, concentrations were deduced and normalized based upon the peak area of the UV signal at 215 nm using a known solution of native ω-CgTx GVIA as the standard. Comparative UV spectra for several of the acetylated derivatives indicated that the absorbance at 274 nm (λ_{max} Tyr) was in good agreement with the 215-nm data. The differential displacement profiles obtained indicate that successive additions of acetyl moieties lead to a loss of activity (i.e., triacetylated < diacetylated < monoacetylated). Within the monoacetylated series, modification of the α-NH_2 of Cys-1 resulted in a significant decrease in binding affinity whereas derivatization of the ϵ-NH_2 of either Lys-2 or Lys-24 had minimal or no effect, respectively. For the diacetylated derivatives, acetylation of Lys-24 and the N-terminus led to the greatest loss in binding affinity. The triacetylated peptide was the least active of all derivatives and showed about a 100-fold decrease in potency versus native ω-CgTx GVIA.

A similar functional profile was obtained for the acetylated derivatives when their ability to inhibit K^+-stimulated $^{45}Ca^{2+}$ influx into chick brain synaptosomes was measured (Table I). Due to limited sample quantities, single doses of either 0.1 or 1 μM were analyzed, and complete concentration response curves were not performed. As shown, successive additions of acetyl moieties led to a decrease in functional potency. Again, acetylation of the N-terminus resulted in the greatest loss of activity within the monoacetylated series.

DISCUSSION

Acetylation of ω-CgTx GVIA, under the reaction conditions stated, generated seven distinct derivatives. Three of these derivatives were determined to be monoacetylated, three were diacetylated, and one was triacetylated. Additional structural studies, using tryptic digestion and FAB-MS, confirmed that these derivatives were formed as a result of an electrophilic attack upon primary amines by acetic anhydride. Attack at other potentially reactive nucleophilic sites, such as tyrosyl and cysteinyl residues, did not occur. As expected, none of the six cysteine residues were available for derivatization since the three disulfide bridges found in the native confirmation were maintained. Circular dichroism measurements for the native vs mono-, di-, and triacetylated derivatives also indicated that no major perturbation of the secondary structure occurred as a result of modification (data not shown). As discussed, retention of the disulfide bonds during tryptic digestion was critical to the isolation of a single RP-HPLC peak for FAB-MS and positional assignment.

The biological ramification of these structural alterations supports our previous observations (Keith et al., 1990) that primary amino groups are important to the function of ω-CgTx GVIA. As reported, successive acetylations of ω-CgTx GVIA led to a decrease in binding affinity and functional potency. Preliminary in vivo data also indicate that the triacetylated species is without effect, and the diacetylated derivatives less effective than either the mono or the native species in inducing tremors or convulsions following ICV injections into mice (J. Patel, ICI Pharmaceuticals, personal communication). Additionally, this loss of activity is sequence-specific and not simply due to nonselective steric hindrance or lowering of basicity since significant differences were determined within the monoacetylated series. This observation is not unexpected

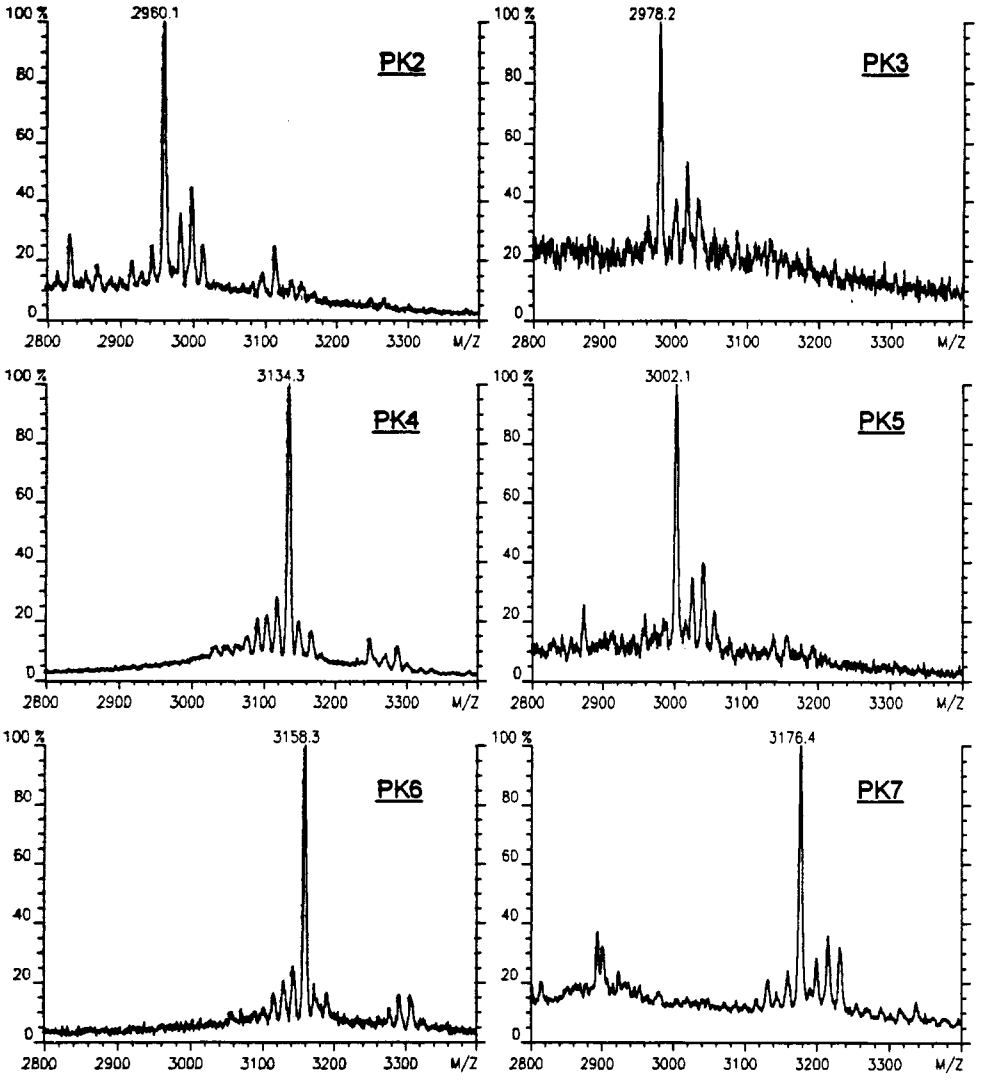

FIGURE 4: Positive ion FAB mass spectra of RP-HPLC peaks 2–7 from Figure 1 following tryptic digestion. The mass signal is expressed as the relative intensity along the y axis.

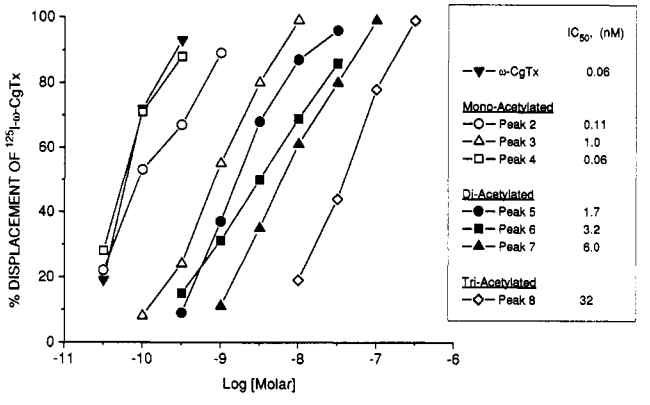

FIGURE 5: Displacement of ^{125}I-ω-CgTx GVIA binding by acetylated derivatives. Each point is the mean of duplicate values which were derived from triplicate samples. SEM are less than 5% for all points.

due to the high degree of secondary structure implied by the three disulfide bridges. Specifically, the α-NH_2 of Cys-1 appears to be a larger determinant in the recognition site of ω-CgTx GVIA than the ϵ-NH_2 of either Lys-2 or Lys-24. N-Terminus extension experiments, in conjunction with amino acid substitutions involving Lys-2 and Lys-24, would help to address this issue.

In conclusion, these data demonstrate that selective modifications of the primary amines of ω-CgTx GVIA can be performed. More importantly, these modifications can be structurally confirmed using a scheme of tryptic digestion followed by FAB-MS to ascertain their biological relevancy. Using these tools, we can further explore the SAR of ω-CgTx GVIA interaction with VDCC. It is felt that this approach will lead to the development of a reversible but still selective ω-CgTx GVIA ligand which can be utilized for future pharmacological studies.

Table I: Inhibition of $^{45}Ca^{2+}$ Influx into Chick Synaptosomes by Acetylated ω-CgTx GVIA Derivatives[a]

compound	% inhibition	compound	% inhibition
ω-CgTx GVIA (0.1 μM)	92 ± 3	peak 5 (1 μM)	48 ± 3
peak 2 (0.1 μM)	44 ± 4	peak 6 (1 μM)	32 ± 8
peak 3 (0.1 μM)	22 ± 6	peak 7 (1 μM)	54 ± 3
peak 4 (0.1 μM)	51 ± 10	peak 8 (1 μM)	5 ± 2

[a] Each value represents the mean of duplicate samples performed in triplicate.

ACKNOWLEDGMENT

We acknowledge the contributions of Dr. Prudence Bradley for assistance with CD measurements and Dr. Jay Patel for helpful discussions.

REFERENCES

Abe, T., Koyano, K., Suisu, H., Nishiuchi, Y., & Sakakibara, S. (1986) *Neurosci. Lett. 71*, 203.

Aosaki, T., & Kasai, H. (1989) *Pflugers Arch. 414*, 150.

Cruz, L. J., & Olivera, B. M. (1986) *J. Biol. Chem. 261*, 6230.

Cruz, L. J., Johnson, D. S., & Olivera, B. M. (1987) *Biochemistry 26*, 820.

Cruz, L. J., Johnson, D. S., Imperial, J. S., Griffin, D., LeCheminant, G. W., Miljanich, G. P., & Olivera, B. M. (1988) *Curr. Top. Membr. Transp. 33*, 417.

Dooley, D. J., Lupp, A., & Hertting, G. (1987) *Naunyn-Schmiedeberg's Arch. Pharmacol. 336*, 467.

Hirning, L. D., Fox, A. P., McCleskey, E. W., Olivera, B. M., Thayer, S. A., Miller, R. J., & Tsien, R. W. (1988) *Science 239*, 57.

Kasai, H., Aosaki, T., & Fukuda, J. (1987) *Neurosci. Res. 4*, 228.

Keith, R. A., Mangano, T. J., Pacheco, M. A., & Salama, A. I. (1989) *J. Auton. Pharmacol. 9*, 243.

Keith, R. A., LaMonte, D., & Salama, A. I. (1990) *J. Auton. Pharmacol. 10*, 139.

Keith, R. A., Mangano, T. J., DeFeo, P. A., Horn, M. B., & Salama, A. I. (1992) *J. Mol. Neurosci. 3*, 147.

Knaus, H. G., Striessnig, J., Koza, A., & Glossmann, H. (1987) *Naunyn-Schmiedeberg's Arch. Pharmacol. 336*, 583.

McCleskey, E. W., Fox, A. P., Feldman, D. H., Cruz, L. J., Olivera, B. M., Tsien, R. W., & Yoshikami, D. (1987) *Proc. Natl. Acad. Sci. U.S.A. 84*, 4327.

Mintz, I. M., Venema, V. J., Swiderek, K. M., Lee, T. D., Bean, B. P., & Adams, M. E. (1992) *Nature 355*, 827.

Nishiuchi, Y., Kumagaye, K., Noda, Y., Watanabe, T. X., & Sakakibara, S. (1986) *Biopolymers 25*, S61.

Olivera, B. M., McIntosh, J. M., Cruz, L. J., Luque, F. A., & Gray, W. R. (1984) *Biochemistry 23*, 5087.

Olivera, B. M., Gray, W. R., Zeikus, R., McIntosh, J. M., Varga, J., Rivier, J., de Santos, V., & Cruz, L. J. (1985) *Science 230*, 1338.

Plummer, M. R., Logothetis, D. E., & Hess, P. (1989) *Neuron 2*, 1453.

Pullan, L. M., Keith, R. A., LaMonte, D., Stumpo, R. J., & Salama, A. I. (1990) *J. Auton. Pharmacol. 10*, 213.

Reynolds, I. J., Wagner, J. A., Snyder, S. H., Thayer, S. A., Olivera, B. M., & Miller, R. J. (1986) *Proc. Natl. Acad. Sci. U.S.A. 83*, 8804.

Stumpo, R. J., Pullan, L. M., & Salama, A. I. (1991) *Eur. J. Pharmacol. 206*, 155.

Suszkiw, J. B., Murawsky, M. M., & Fortner, R. C. (1987) *Biochem. Biophys. Res. Commun. 145*, 1283.

Wagner, J. A., Snowman, A. M., Biswas, A., Olivera, B. M., & Snyder, S. H. (1988) *J. Neurosci. 8*, 3354.

Werth, J. L., Hirning, L. D., & Thayer, S. A. (1991) *Mol. Pharmacol. 40*, 742.